

# Wind Events Compared With Polynya Area Estimates Derived From SSM/I Data

Thorsten Markus and Barbara A. Burns\*

Institute of Remote Sensing  
University of Bremen, FB1  
D-28334 Bremen, Germany

## ABSTRACT

Different methods for estimating ice concentration as well as special polynya detection algorithms are applied to passive microwave data (here SSM/I) to determine the size of small coastal polynyi, in the Weddell Sea region of the Antarctic for September 1989. The detection algorithms use 1- and 2-dimensional polynya signature models (PSM) based on generation of synthetic microwave images of polynya events, which are compared with measured microwave data of the 37 GHz vertical polarization channel. The results from all methods are compared with wind data and with calculations from a dynamic model of polynya size in a case study for a region close to Halley Bay. All passive microwave methods resolve single peaks in the history of the polynya size but differ significantly in absolute area measured and its fluctuation. The 2-D PSM method, presented here for the first time, shows best correlation with wind data (Correlation Coefficient  $CC = 0.78$ ) as well as with the dynamic model ( $CC = 0.80$ ). It has a bias of  $41 \text{ km}^2$  and an rms error of  $173 \text{ km}^2$ . This is very acceptable given the coarse resolution of approximately  $625 \text{ km}^2$  for one SSM/I pixel.

## 1. INTRODUCTION

The importance of Antarctic coastal polynyi for the heat exchange between ocean and atmosphere, for heavy ice production and thus, with the resultant brine rejection, for a large amount of the Antarctic bottom water is widely recognized (e.g. Smith et al.(1990)). To obtain full understanding of their influence continuous detection of even small polynyi is necessary. Only passive microwave sensors with their daily coverage of the polar regions and their low sensitivity to clouds can provide this information. But because of the large size of the sensor footprints, depending on frequency and antenna size, coastal polynyi generally cannot be resolved with brightness temperature

measurements and therefore with normal ice concentration algorithms.

Previous studies using microwave data to estimate polynya area are those of Cavalieri and Martin (1985) and Zwally et al. (1985), both of which use a linear interpolation with the 37GHz vertical polarized (37V) channel to calculate ice concentration, and those of Martin and Cavalieri (1989) and Cavalieri and Martin (1994) which used the NASA Team ice concentration algorithm first described in Cavalieri et al. (1984) and Gloersen and Cavalieri (1986). Polynya areas less than  $1000 \text{ km}^2$  were not resolved in any of these studies.

In order to detect subpixel-scale polynyi with passive microwave data, a polynya signature model was developed. With this method polynya areas of the order of  $100 \text{ km}^2$  and larger can be estimated (Markus and Burns, 1993). In contrast to previous work, no ice concentration calculations are needed. Rather the method is based on simulating the brightness temperature transition from sea ice to shelf ice, with and without a coastal polynya. The models generated are then compared with image data along transects across the coast. The polynya signature method has now been expanded to two dimensions.

In this paper this improved version of this method is compared with the methods previously used as well as an ice concentration algorithm developed by Swift et al. (1985). All methods are applied to SSM/I data for September 1989 to derive polynya area estimates for locations near the Antarctic coast over a period of one month. In particular the sensitivity of these estimation methods for detecting small scale features is investigated.

That coastal polynyi are highly correlated with wind events has been clearly demonstrated (e.g. Cavalieri and Martin (1985), Markus and Burns (1993)). Therefore the results are compared with hourly meteorological data from Hal-

\* Now at CIMSS/Space Science and Engineering Center University of Wisconsin – Madison, U.S.A.

ley station and with a model which describes the development of wind driven coastal polynya (Pease, 1987).

## 2. DATA SETS

The area of study is the eastern coast of the Weddell Sea south of Halley station (Fig. 1). This area is chosen because first it is close to the Halley station and second an ice tongue prevents the pack ice from drifting into the polynya, a necessary condition for the undisturbed formation of polynya (Bromwich and Kurtz, 1984). This area is therefore sheltered from the Weddell Gyre so that in the model of Pease (1987) currents can be neglected.

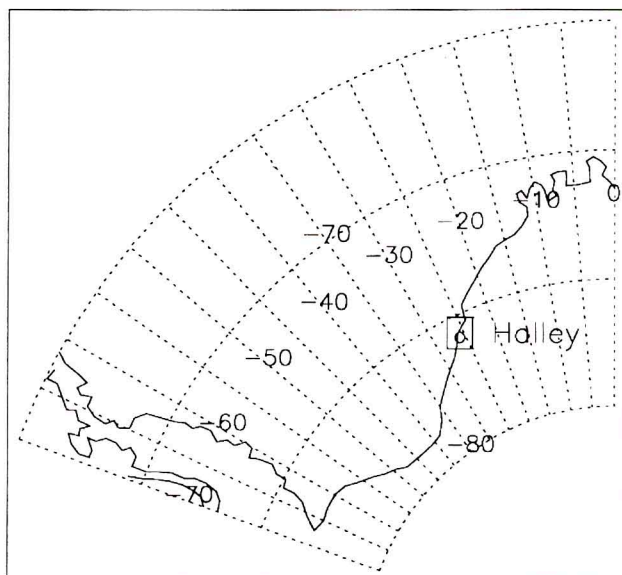


Fig. 1 - Area of Study

The passive microwave data come from the Special Sensor Microwave/Imager (SSM/I) onboard a satellite of the Defense Meteorological Satellite Program (DMSP). The SSM/I provides measurements in seven frequency-polarization channels with a sample spacing of 25 km for the lower frequency channels (19 GHz H+V, 22 GHz V, 37 GHz H + V) and 12.5 km for the 85 GHz H + V channels. The daily-averaged data used here were obtained from NSIDC in Boulder mapped to a polar stereographic projection format on CD-ROM.

Because of the large footprint of the sensor there is always a contribution from land or shelf ice brightness temperature in a pixel near the coast. We therefore also examine different methods of masking out the land. Cavalieri and Martin (1985) and Martin and Cavalieri (1989) exclude all pixels which contain any land or shelf ice. Zwally *et al.* (1985) exclude all pixels where the center of the data ele-

ment lies over land, so that the contribution of land lies between 0 % and 50 % with a mean contribution of 25 %. As a third possibility of masking we resample the data to a 5 km grid with bilinear interpolation and mask out pixels using a 5 km resolution land mask. This of course provides no new information but does preserve as much of the original information as possible.

## 3. DESCRIPTION OF METHODS

### 3.1 Linear Interpolation of Brightness Temperatures

Cavalieri and Martin (1985) determined the size coastal polynya with passive microwave data from the Scanning Multichannel Microwave Radiometer (SMMR) using a linear interpolation of the brightness temperature measured in the 37V channel. The two tiepoints for open water and for 100 % ice were determined with a histogram method. Similar tiepoints were found in this analysis:  $T_{BW} = 200$  K for open water (Cavalieri and Martin 200 K),  $T_{BI} = 250$  K for 100 % ice (245 K). Although the resolution of the SMMR's 37V channel was 27 km x 32 km, because of its high sampling rate they could bring the data into a grid with pixel size (ps) of 15 km x 15 km. Areas along the coast were defined where all pixels containing any land were excluded. The polynya size (surface area) was calculated as

$$A_p = \sum_i (1 - c_i) \cdot ps \quad (1)$$

The sum is over each pixel inside the area with  $c_i$  the respective ice concentration

$$c_i = \frac{T_{Bi} - T_{BW}}{T_{BI} - T_{BW}} \quad (2)$$

and  $T_{Bi}$  the measured brightness temperature averaged over four days.

In order not to include leads or other kinds of ice concentration reductions not associated with the polynya Cavalieri and Martin chose three different polynya area definitions for  $A_p$ :

- the open water contribution from every pixel in the area was taken into account
- All pixels with an ice concentration > 75 % were assumed totally ice covered ( $c_i > 0.75 \rightarrow c_i = 1$ )
- All pixels with an ice concentration > 50 % were assumed totally ice covered ( $c_i > 0.5 \rightarrow c_i = 1$ )



Because the correlation of polynya size with wind data over a relatively long time period was best with the second definition they chose the 75 % cutoff for their calculations. It should be noted that the difference between  $A_{ps}$  with the 50 % and the 75 % definitions was about a factor 6. The polynya sizes were all larger than 1000 km<sup>2</sup>.

### 3.2 NASA Team Ice Concentration Algorithm

In the studies of Martin and Cavalieri (1989) and Cavalieri and Martin (1994) ice concentration is calculated following Cavalieri et al. (1984). This algorithm (NASA Team) makes use of both frequency and polarization information at 19 and 37 GHz. Determination of ice concentration is based on the fact that at 19 GHz the polarization of open water is much greater than that of ice and the spectral gradient ratio is positive for open water and near below zero for ice.

The ice concentration is given by

$$c = \frac{A_1 (GR) + A_2 (GR) \cdot PR}{A_3 (GR) + A_4 (GR) \cdot PR} \quad (3)$$

where the spectral gradient ratio (GR) is defined as

$$GR = \frac{T_{BV}(37) - T_{BV}(19)}{T_{BV}(37) + T_{BV}(19)} \quad (4)$$

and the polarization ratio (PR) is given by

$$PR(v) = \frac{T_{BV}(v) - T_{BH}(v)}{T_{BV}(v) + T_{BH}(v)} \quad (5)$$

with  $T_{BV}$  and  $T_{BH}$  the observed vertical and horizontal polarized brightness temperatures and  $\nu$  is either 19 or 37 GHz. Operationally the 19 GHz channel is used. This is supported by Steffen and Maslanik (1988) who showed that results from the algorithm with PR ( $\nu = 19$  GHz) are best correlated with high resolution Landsat data. The  $A_i$  are functions of fixed tiepoints for ice and open water as well as the multiyear ice fraction which is determined primarily from the measured GR value.

In both Martin and Cavalieri (1989) and Cavalieri and Martin (1994) polynya size is calculated similarly to Cavalieri and Martin (1985) using equation (1) with the first definition where all pixels contribute. In our case the pixel size (ps) is 25 km x 25 km.

Cavalieri and Martin (1994) discuss two sources of error for polynya size estimates. The first is the influence of land

due to the large footprint. They found that for a large polynya the difference between pixels with low ice concentration far from the coast and pixels close to the land is generally smaller than 10 %, so that the error due to land is assumed to be small. But this still leads to an underestimation of ice concentration or equivalently an overestimation of polynya area. The second error source results from the inability of the NASA Team algorithm to discriminate young ice which is interpreted as a mixture of open water and first-year ice. This results in an additional systematic overestimation of open water.

### 3.3 Ice Concentration Algorithm of Swift et al. (1985)

This algorithm is based on deriving emissivity ( $\epsilon$ ) from the brightness temperature data using a simplification of the radiative transfer equation :

$$T_B(v) - A(v, \tau, T_{air}) = \epsilon(v)(\tau(v) \cdot T_S - B(v, \tau, T_{air})) \quad (6)$$

where  $\nu$  is the frequency channel (19 or 37 GHz, V-pol),  $A$  and  $B$  are functions of the atmospheric opacity  $\tau$  and surface air temperature  $T_{air}$ .  $T_B$  is the measured brightness temperature and  $T_S$  the temperature of the emitting surface, which is calculated from the air temperature after Comiso et al. (1989):

$$T_S = -3.2 + 0.237 T_{air} + 273.15 \quad (7)$$

The emissivity is assumed to be a composite of the emissivities of open water ( $\epsilon_W$ ), first-year ice ( $\epsilon_{FY}$ ) and multiyear ice ( $\epsilon_{MY}$ )

$$\epsilon = f_W \epsilon_W + f_{FY} \epsilon_{FY} + f_{MY} \epsilon_{MY} \quad (8)$$

where  $f_i$  is the fraction of surface type  $i$ . Because  $\sum_i f_i = 1$  one fraction can be eliminated

$$\epsilon = \epsilon_{FY} - f_W(\epsilon_{FY} - \epsilon_W) - f_{MY}(\epsilon_{FY} - \epsilon_{MY}) \quad (9)$$

The tiepoints, i.e emissivities, for the three surface types are derived from the data to account for variations in surface conditions. As they show little deviation for the month of data under study they are assumed to be constant.

Simultaneous solution of equations (6) and (9) provides an expression for  $f_W$  and  $f_{MY}$  in terms of the emissivity tie points and measured brightness temperatures. The ice concentration is then given by:

$$c = 1 - f_W \quad (10)$$

The polynya size  $A_p$  is calculated as before by summing up the open water concentration multiplied by the pixel size using contributions from all pixels in the defined area.

### 3.4 1-D Polynya Signature Model (PSM) Method

This method, described in Markus and Burns (1993), was developed to obtain surface area estimates for sub-pixel size polynya with SSM/I data. It is based on a simulation of the brightness temperature transition across a polynya, from the pack ice and onto the shelf ice, as would be measured by a satellite-borne radiometer. This avoids a weak point in the linear interpolation method where the brightness temperature of the shelf ice is not accounted for.

Synthetic images at 5 km pixel spacing are generated for cases with polynya widths of 1, 3 and 5 km and without a polynya using average brightness temperatures values of sea ice, open water and shelf ice taken from the measured 37 GHz vertical polarization data. Brightness temperatures vary in only one dimension in these images (perpendicular to the coast) and are constant in the orthogonal dimension. Satellite data are simulated by convolving the images a rotationally symmetric Gaussian antenna pattern with the beamwidth characteristic of the SSM/I sensor. Profiles through these simulated data are then compared with the measured data, which are resampled to a 5 km grid using bilinear interpolation.

To decide if a pixel contains open water the correlation between profiles through the four models (simulated data with and without polynya) and a profile through the 37V data centered at the pixel in question is calculated. The pixel is detected as an ‘open water’ pixel if the correlation coefficient is nearer one for one of the cases with polynya than for the case without. The contribution to  $A_p$  is 5, 15 or 25 km<sup>2</sup> for the assumed polynya widths of 1, 3 and 5 km, respectively. 1 km is the minimum polynya width where the models show any difference. The total polynya area is calculated from the contribution from each detected 5 km pixel.

To reduce the number of pixels for which correlation coefficients must be calculated, the 85H channel, with its higher spatial information, is used to make a predetection. (Note that although the vertical polarization would be preferred, only the horizontal channel was available in our data set.) Only those pixels are taken into consideration for which the brightness temperature is below a threshold value calculated to account for the influence of open water as well as the variability of shelf ice.

Although shelf ice variability and weather effects can lead to false predetections with the 85H channel, these errors are mostly corrected with the use of the 37V channel in the final detection process. This channel is largely free from weather effects and much less sensitive to physical inhomogeneities in the surface layer than both 85 and 37 horizontal polarization channels. Test applications have also shown the higher resolution at 37 GHz to be more important than the higher water-ice contrast at 19 GHz.

The algorithm can be summarized in the following steps:

1. Interpolate data to 5 km grid
2. Predetect pixels with 85H threshold
3. Correlate model with 37 GHz data for every predetected pixel to detect pixels with open water
4. Sum open water contributions of detected pixels

### 3.5 2-D Polynya Signature Model (PSM) Method

The 1-D PSM method described above assumes a linear polynya with an effective length equal to that of the beamwidth of the antenna pattern and does not account for the shape of coastline and polynya. Therefore the method performs very poorly for nonlinear polynya because the entire data profile might lie within an area of open water. In this paper the method is expanded to include a two-dimensional model to avoid these problems.





Again the predetection is made using the 85H channel. The data are bilinear interpolated into a 5 km grid and a land/shelf mask applied. The coast is divided into several boxes which are analysed separately to minimize the effect of shelf ice and cloud cover variability. The minimum pixel value outside the land/shelf ice area ( $T_{Bmin}$ ) is determined and all pixels with a  $T_B$  below  $T_{Bmin} + \Delta T$  form the possible polynya. The value of  $\Delta T$  must be high enough to overestimate the polynya size on the first step.

A synthetic image is then generated by assigning the predetected pixels the  $T_B$  of open water, the sea ice pixels the mean  $T_B$  of sea ice and the land/shelf ice pixels the mean  $T_B$  of shelf ice, with all values taken from the 37V data in the box and for the day in question. This image is convolved with the antenna pattern as described above creating simulated 37V data with 25-km pixel spacing to match the sample spacing of the SSM/I data. A 2-D correlation between the simulated and the measured 37V image data is then calculated.



These three steps (predetection, image simulation and 2-D correlation) are repeated, each time reducing the value of  $\Delta T$  in the predetection step, and thereby reducing the number of 'polynya pixels', until the best correlation is found. The polynya area is then calculated by multiplying the number of predetected pixels in the 85 GHz image that resulted in the best correlation by the pixel size, i.e. 25 km<sup>2</sup>.

Figure 2 show for the whole month the pixels predetected in the first step overlain with the pixels finally detected. On most days the first guess closely approximates the area finally detected. However on September 22 the area detected in the first iteration is much larger which is probably due to the influence of clouds. Clouds result in higher brightness temperatures at 85 GHz and thus a higher  $T_{Bmin}$ , possibly close to that of sea ice. This produces a large overestimate of polynya area at the predetection step in the first iteration. However this area will be reduced since final detection depends on the correlation at 37 GHz. As will be shown in Section 6 the area finally detected on September 22 is reasonable size. Thus by using the 85 GHz for the predetection only, its higher spatial information is utilized but the influence of cloud is less important than if this frequency were used alone.

	sea ice		detected pixels
	shelf ice		predetected pixels

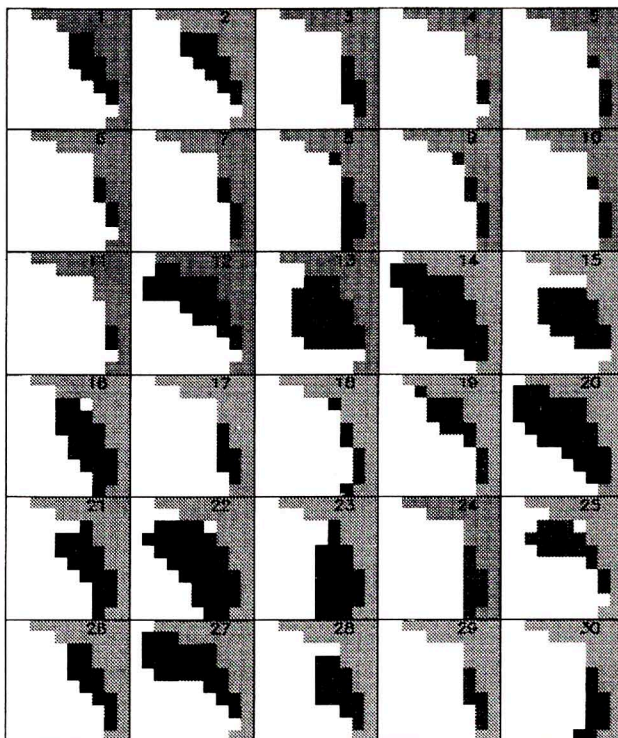


Fig. 2 - Predetected (in the first step) and detected pixels using the 2-D PSM for the whole month.

#### 4. RESULTS

The different methods described above are applied to the daily averaged SSM/I data of September 1989. Figure 3 shows the polynya area results as well as the daily average wind speed perpendicular to the coast (Fig. 3f) at Halley Bay. On first sight the difference between results from the various methods seems to be very large but a difference in ice concentration of 10 % results in a difference for a single pixel of about 60 km<sup>2</sup>. So the largest difference between the NASA (Fig. 3b) and the Swift et al. (Fig. 3c) algorithm of about 350 km<sup>2</sup> can easily be reached with more pixels taken into consideration.

In the result from the linear interpolation method of Cavalieri and Martin (1985) (Fig. 3a) the maximum polynya area on September 13 and also the peaks on September 22, 25 and 27 are in agreement with the wind data. But there is a striking difference in mean open water area between the first and the second half of the month. Comparison with the mean brightness temperatures of the shelf ice at 37 GHz also shown in Fig. 3a suggests that the open water area is highly dependent on the brightness temperature of the shelf ice. For example on September 17 where  $T_B(\text{shelf})$  has a maximum the polynya area has a minimum and conversely the mean  $T_B(\text{shelf})$  is lower for the first half of the month than for the second which corresponds well with the larger mean polynya area for the first half. The shelf ice brightness temperatures appear to be highly correlated with the mean air temperatures with a lag of about two days.

The effect of using different methods of masking out land area is also demonstrated in Fig. 3a-c. Whereas the occurrence of individual peaks is unaffected, the absolute size changes significantly. The method of masking out all pixels containing any land is clearly too crude for small scale events. The bilinear interpolation method and the method of masking out pixels with more than 50 % land are similar especially for the Swift et al. and NASA algorithm. For quantitative comparisons between the ice concentration and polynya signature methods, the bilinear interpolation method was used in all cases.

In Fig. 3b the results using the NASA team algorithm are presented. Except for the peak on September 14 and the minimum on September 18 there is little correlation seen with the wind data. Analysis of the single channels used in the algorithm showed that the 19H channel is mainly responsible for differences with wind data and the other algorithms, for example the overly large area around September 21 and the peaks on September 26 and 28, which

fall on September 25 and 27 in all the other methods. The reason, as mentioned above, is that the NASA algorithm interprets young ice as a mixture of ice and open water, whereas other algorithms interpret it as ice only (Burns, 1993). This is because young ice has a signature between open water and first-year ice at 19H, but is very similar to first-year ice at 19V and at 37 GHz (Grenfell, 1986).

Fig. 3c presents the results of the algorithm by Swift *et al.* Qualitatively the peaks on the single days mentioned above are seen here as well, but their excess over neighbouring

days is much reduced. The overall larger polynya area in comparison with the NASA algorithm is in agreement with the results by Burns(1993) which show lower ice concentration for locations near the coast for the Swift *et al.* algorithm than for the NASA team algorithm.

In Fig. 3d and 3e the polynya areas obtained using the 1-D and 2-D polynya signature models (PSM) are shown. Here even a small increase in wind speed, e.g. September 7, shows a corresponding increase in the polynya area, especially the peaks for the second half of the month. Also

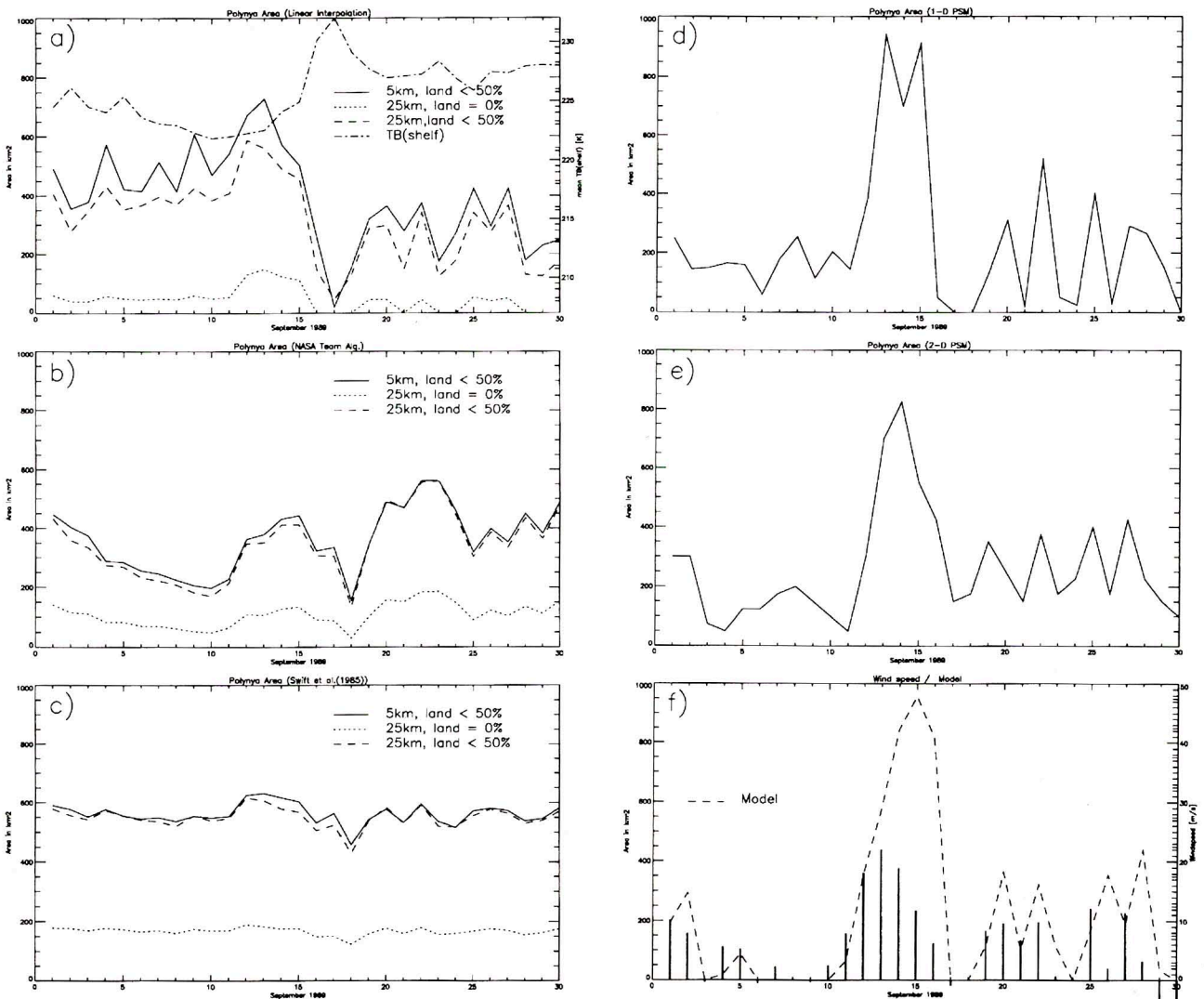


Fig. 3 - Polynya areas for September 1989 with different methods and different methods of masking out land:

a : Linear Interpolation and Mean brightness temperature of the shelf ice in 37V

b : Algorithm from Swift *et al.*

c : NASA Team algorithm

d : 1-D PSM

e : 2-D PSM

f : Wind speed perpendicular to the coast (Arrows) and model results.



the sizes correspond well with wind speed. The relatively large area on September 30 in the 2-D PSM and in the ice concentration methods where no polynya is expected from wind data is due a polynya forming off Coats Land which extends into the southern portion of our area of study (see Fig. 2). This is confirmed with AVHRR data for that day described by Markus and Burns (1993).

Table 1 shows the correlation coefficients for the different passive microwave methods with the wind data. Because all peaks in wind speed are seen in the Swift et al. algorithm result, it has a high correlation coefficient although the overall area is very large with little variation.

**Table 1 – Correlation Coefficients of passive microwave methods with wind data.**

Algorithm	Lin. Interp.	Swift et al.	NASA 1-D PSM	2-D PSM	
Corr.-Coeff.	0.598	0.767	0.331	0.783	0.785

## 5. THERMODYNAMIC-DYNAMIC MODEL OF POLYNIA WIDTHS

Because the size of wind-driven coastal polynya depends not only on wind but on temperature as well the model by Pease (1987) is implemented.

In this model the polynya width ( $X_p$ ) is determined by the advection rate of the ice ( $V_i$ ) and the ice production rate ( $F_i$ ) as

$$\frac{dX_p}{dt} = V_i - \frac{X_p F_i}{H_i} \quad (11)$$

where  $H_i$  is the collection depth of grease ice or nilas which is assumed to be constant at 0.1 m. The advection rate is assumed to be 3 % of the wind speed component perpendicular to the coast ( $V_a$ ).

The ice production is given by

$$F_i = \frac{H_{tot}}{\rho_i L} \quad (12)$$

where  $\rho_i = 0.95 \cdot 10^3 \text{ kg m}^{-3}$  is the density of young saline sea ice,  $L = 3.34 \cdot 10^5 \text{ J kg}^{-1}$  is the latent heat of freezing salt water and  $H_{tot}$  is the total heat flux.

The total heat flux is given by

$$H_{tot} = Q_t + Q_e + Q_{lu} - Q_{ld} - Q_s$$

The first three terms, i.e. the turbulent heat flux ( $Q_t$ ), the evaporative heat flux ( $Q_e$ ) and the longwave radiation emitted from the surface ( $Q_{lu}$ ) are directed from the surface layer to the atmosphere. The last two terms, i.e. the downward longwave radiation ( $Q_{ld}$ ) and the solar radiation ( $Q_s$ ) are oppositely directed from the atmosphere into the surface layer. For temperatures below freezing  $Q_t$  and  $Q_e$  have the same sign. With decreasing temperatures  $Q_t$  is more and more dominating, so that at temperatures of  $-10^\circ\text{C}$   $Q_e$  is smaller than the uncertainty of  $Q_t$  and is therefore neglected in the following calculations (Pease, 1987).  $Q_{lu}$  is a function of air temperature only and  $Q_t$  of air temperature and wind speed, whereas  $Q_{ld}$  and  $Q_s$  are functions of cloud cover fraction (CI) among other parameters and  $Q_s$  additionally of the relative humidity.

The single terms are calculated following Maykut (1985) and, for the solar radiation, Parkinson and Washington (1979). The cloud cover fraction and relative humidity are not known for this study. The effect of cloud cover on the total heat balance can be up to  $150 \text{ W m}^{-2}$  whereas calculations show that different relative humidities have no significant influence on the solar radiation and therefore on the total heat balance. However deviations of the over polynya wind speed and air temperature from values measured at the station can result in errors in sensible heat flux about 32 % (Cavalieri and Martin, 1992).

Fig.4 presents the hourly polynya areas derived with the model. It shows that there is a large variation of polynya area within a single day but which cannot be resolved with the daily averaged SSM/I data. For comparison with the microwave results 24-hour averages are formed.

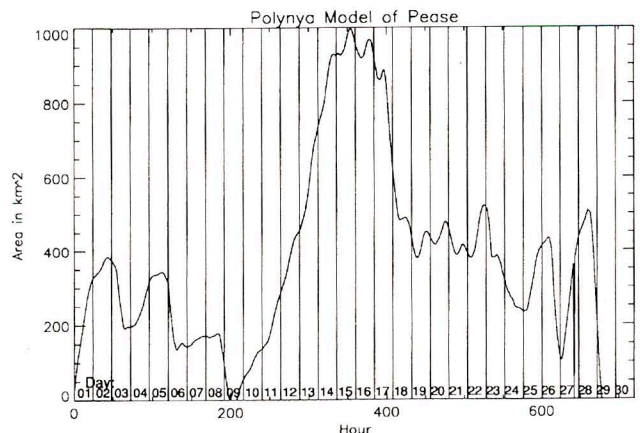


Fig. 4 - Hourly polynya areas based on the Pease (1987) model calculations

### 5.1 Modifications to the Pease Model

Comparison of Fig.3 (a-e) and 4 shows that the temporal change of polynya size predicted by the Pease model is quite similar to the passive microwave results, except for the decrease after the maximum in the middle of the month. In the model the large polynya refreezes exponentially slower with decreasing polynya width and thus influences the predicted polynya area for the entire remainder of the month. This results from the fact that for small wind speeds, as on September 17 and 18, the differential equation of polynya width is not valid and underestimates the time of refreezing. Pease indicated that the wind speed at which the equation fails might be around 5 m/s. We therefore introduce a wind speed cut-off below which no advection takes place and assume uniform refreezing at the ice production rate  $F_i$ . For comparison with microwave results we also have to decide at which ice thickness the polynya is said to be closed, which might be slightly higher than 0.02 m (Grenfell, 1986). Because both the wind speed cut-off and the ice thickness cut-off are uncertain we have examined with wind speed cut-offs of 2, 5 and 7 m/s and ice thickness cut-offs of 0.02, 0.03 and 0.05 m.

The modified model is applied with different cut-offs in wind speed and ice thickness ( $Th$ ) as well as with two dif-

ferent cloud cover fractions (0.8 and 1.0). The results with a wind speed cut-off of 2 m/s closely resemble the original model. Comparing time series with the 5 and 7 m/s wind speed cut-offs, two major differences should be mentioned. First the minimum area after the peak on September 15 (Fig. 4) shifts to September 18 and 19 respectively. So a lag of one day results. Second with decreasing wind speed the 7 m/s cut-off is reached earlier which results in minor minima not seen using the 5 m/s cut-off. The effect of the ice thickness cut-offs depends mainly on the total heat flux during times of low wind speed. It is also dependent on the continuance of wind speed below the respective wind-speed cut-off. Therefore it has different effects depending on the other parameters and on the freezing rate on the respective day.

## 6. COMPARISON WITH MICROWAVE DATA RESULTS

Table 2 shows the correlation coefficients for the different passive microwave methods with the model results with different parameters, i.e wind speed cut-off, ice thickness cut-off and cloud cover fraction.

**Table 2 - Correlation coefficients of passive microwave methods with model results using different parameters.**

Lin. Interp.	Correlation Coefficients				Model Parameter		
	Swift et al.	NASA	1-D PSM	2-D PSM	V [m/s]	Th [m]	CL
-0.22	0.22	0.23	0.39	0.54	2	0.02	1.0
-0.12	0.45	0.38	0.47	0.64	5	0.02	1.0
0.19	0.52	0.42	0.68	0.80	7	0.02	1.0
-0.31	0.15	0.31	0.36	0.60	2	0.03	1.0
-0.21	0.37	0.43	0.43	0.61	5	0.03	1.0
0.15	0.50	0.42	0.64	0.79	7	0.03	1.0
-0.31	0.15	0.31	0.36	0.60	2	0.05	1.0
-0.34	0.10	0.25	0.31	0.52	5	0.05	1.0
-0.13	0.45	0.41	0.48	0.65	7	0.05	1.0
-0.38	0.07	0.27	0.29	0.55	2	0.02	0.8
-0.15	0.42	0.36	0.45	0.62	5	0.02	0.8
0.16	0.49	0.40	0.64	0.78	7	0.02	0.8
-0.38	0.07	0.27	0.29	0.55	2	0.03	0.8
-0.25	0.33	0.42	0.40	0.59	5	0.03	0.8
0.10	0.46	0.34	0.49	0.67	7	0.03	0.8
-0.38	0.07	0.27	0.29	0.55	2	0.05	0.8
-0.45	-0.04	0.31	0.20	0.51	5	0.05	0.8
-0.21	0.36	0.37	0.42	0.62	7	0.05	0.8



The best correlation is found for the 2-D PSM (a coefficient of 0.80) with model parameters wind speed cut-off = 7 m/s, ice thickness cut-off = 0.02 m and cloud cover fraction = 1.0. The model calculations with these parameters also have the best or second best correlations with all the other passive microwave methods.

This model is used as a basis for intercomparison of microwave results and is shown in Fig. 3f. The daily difference between microwave-derived and model polynya area (method – model) are shown for the whole month in Fig. 5. As expected from the correlation analysis, the difference is smallest for the 2-D PSM. But there is a strikingly large difference for all methods at September 16. This results because in the PM results the polynya reaches its maximum size (September 13) earlier than the model does (September 15). This discrepancy is also seen for the peaks in wind data and passive microwave methods for September 25 and 27, whereas in the model these peaks are on September 26 and 28. This error might result from the assumption in the Pease model of an infinite surface drift by which the frazil ice is formed in the open ocean and is advected downwind and collected at the ice edge, as assumed in the Pease model. The incorporation of a finite surface drift would accelerate the adjustment of the ice edge to its final equilibrium (Ou, 1988).

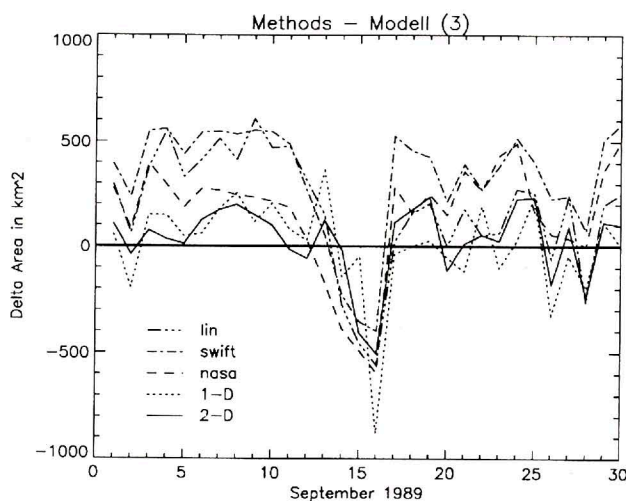


Fig. 5 - Differences between microwave results and model calculations (Parameters: Wind speed = 7 m/s; Th = 0.02 m; Cl = 1.0)

Table 3 gives an overview of the agreement of the different microwave methods with the model using various criteria. The correlation is best with the 2-D PSM. The ice concentration algorithms have a high positive bias, that is on average they overestimate polynya area. This results from the fact that the ice concentration does not reach 100 % because of leads and, as mentioned in section 3.2,

the influence of land inside a pixel, which reduces the ice concentration. Therefore a small polynya is always detected. The 1-D PSM shows no significant bias whereas the 2-D PSM overestimates the polynya area slightly over the whole month. The rms difference of polynya area between model and passive microwave methods is smallest with the 2-D PSM closely followed by the 1-D PSM.

**Table 3 - Comparison of passive microwave results with the model using a wind speed cut-off of 7 m/s, ice thickness cut-off = 0.02 m and cloud cover fraction = 1.0.**

	Lin.	Inter.	Swift et al.	NASA	1-D PSM	2-D PSM
Correlation Coefficient	0.19		0.53	0.42	0.68	0.80
BIAS [km <sup>2</sup> ]	172.5		334.0	149.2	17.4	41.1
RMS difference [km <sup>2</sup> ]	336.4		421.2	289.4	209.4	173.5

## 7. CONCLUSIONS

Polynya area estimates derived from passive microwave methods generally show good agreement with calculations from a dynamic model of polynya size and wind data. The linear interpolation method resolves individual peaks but estimation of absolute area could be much improved by taking into account the influence of the adjacent shelf ice or land. The NASA Team algorithm shows some disagreements which probably result from young ice when a polynya is refrozen and from the sensitivity of the 19H channel to surface features. The algorithm of Swift et al. shows good resolution of single peaks which is expressed through the high correlation with wind data and model results, but the overall too large area and the lack of variation might result from the coarse resolution of 19V channel which is mainly used for the ice concentration estimates. In the NASA algorithm this effect is compensated by combination with 37 GHz and the high open water-sea ice contrast at 19H. The 1-D and 2-D polynya signature model methods show the best results. The 2-D PSM has the highest correlation coefficients and smallest rms difference although the bias is slightly higher than for the 1-D PSM. The correspondence between microwave results and meteorological observations also suggests that the application of the simple model from Pease (1987) is quite suitable for polynya width calculations although rough assumptions for ice advection rate and oceanic heat flux must be made. The incorporation of a finite surface drift as mentioned in the previous section and of course the knowledge of the cloud cover fraction should improve the results.

## ACKNOWLEDGEMENTS

We want to thank John King from the British Antarctic Survey for the meteorological data from Halley Station and the DFG for the financial support of this project.

## REFERENCES

- Bromwich H.B. & Kurtz D.D., 1984, Katabatic Wind Forcing of the Terra Nova Bay Polynya, *J. Geophys. Res.*, Vol.89, No.63, 3561-3572.
- Burns B.A., 1993, Comparison of SSM/I Ice Concentration Algorithms for the Weddell Sea, *Annals of Glaciology*, 17, 344-350.
- Cavalieri D.J., Gloersen P. & Campbell W.J., 1984, Determination of Sea Ice Parameters With the NIMBUS 7 SMMR, *J. Geophys. Res.*, 89, 5355-5369.
- Cavalieri D.J. & Martin S., 1985, A Passive Microwave Study of Polynyas Along the Antarctic Wilkes Land Coast, *Oceanology of the Antarctic Continental Shelf, Ant. Res. Ser.*, Vol.43.
- Cavalieri D.J. & Martin S., 1994, The Contribution of Alaskan, Siberian and Canadian Coastal Polynyas to the Cold Halocline Layer of the Arctic Ocean, *J. Geophys. Res.*, vol. 99, 18, 343-18, 362.
- Comiso J.C. & Sullivan C.W., 1986, Satellite Microwave And In Situ Observations of the Weddell Sea Ice Cover And Its Marginal Ice Zone, *J. Geophys. Res.*, 91, 9663-9681.
- Comiso J.C., Grenfell T.C., Bell D.L., Lange M.A. & Ackley S.F., 1989, Passive Microwave In Situ Observations of Winter Weddell Sea Ice, *J. Geophys. Res.*, 94, 10891-10905.
- Gloersen P. & Cavalieri D.J., 1986, Reduction of Weather Effects in the Calculation of Sea Ice Concentration From Microwave Radiances, *J. Geophys. Res.*, 91, 3913-3919.
- Grenfell T.C., 1986, Surface-Based Passive Microwave Observations of Sea Ice in the Bering Sea and Greenland Seas, *IEEE Transactions on Geoscience and Remote Sensing*, Vol. GE-24, No.3.
- Markus T. and Burns B.A., 1993, Detection of Coastal Polynyas With Passive Microwave Data, *Annals of Glaciology*, 17, 351-355.
- Martin S. & Cavalieri D.J., 1989, Contributions of the Siberian Shelf Polynyas to the Arctic Ocean Intermediate and Deep Water, *J. Geophys. Res.* Vol. 94, C9, 12, 725-12, 738.
- Maykut G.A., 1985, An Introduction to Ice in the Polar Oceans, *APL-UW* 8510.
- Ou Hsien Wang, 1988, A Time-Dependent Model of a Coastal Polynya, *J. Phys. Oceanography*, Vol. 18, 584-590.
- Parkinson C.L. & Washington W.M., 1979, A Large-Scale Numerical Model of Sea Ice, *J. Geophys. Res.*, Vol. 84, C1, 311-337.
- Pease C.H., 1987, The Size of Wind-Driven Coastal Polynyas, *J. Geophys. Res.*, Vol. 92, No.C7, 7049-7059.
- Smith S.D., Muench R.D. & Pease C.H., 1990, Polynyas and Leads: An Overview of Physical Processes and Environment, *J. Geophys. Res.*, Vol. 95, No. C6, 9461-9479.
- Steffen K. & Maslanik J.A., 1988, Comparison of Nimbus 7 Scanning Multichannel Microwave Radiometer Radiance And Derived Sea Ice Concentrations With Landsat Imagery for the North Water Area of Baffin Bay, *J. Geophys. Res.*, 93, C9, 10769-10781.
- Swift C.T., Fedor L.S. & Ramseier R.O., 1985 An Algorithm to measure Sea Ice Concentration With Microwave Radiometers, *J. Geophys. R.*, 90, 1087-1099.
- Zwally H.J. & Comiso J.C., 1985, Antarctic Offshore Leads And Polynyas And Oceanographic Effects, *Oceanology of the Antarctic Continental Shelf, Ant. Res. Ser.*, Vol.43.